Polymer Degradation and Stability 246 (2026) 111949

Contents lists available at ScienceDirect

Polymer Degradation and Stability

journal homepage: www.journals.elsevier.com/polymer-degradation-and-stability

From simulation to distribution: A novel approach to depolymerization kinetics using PHB hydrolysis as a case study

Norbert Hohenauer [a,b], Dominik Wielend [a], Katharina Kelderer [a], Jan-Michael Holzinger [c], Gunnar Spiegel [a], Clemens Schwarzinger [b], Christian Paulik [a,b,*]

[a] Competence Center CHASE GmbH, Hafenstrasse 47–51, Linz, 4020, Austria
[b] Institute for Chemical Technology of Organic Materials, Johannes Kepler University Linz, Altenberger Strasse 69, Linz, 4040, Austria
[c] Linz School of Education, Department MINT Didaktik, Johannes Kepler University Linz, Altenberger Strasse 69, Linz, 4040, Austria

ARTICLE INFO

Keywords:
Depolymerization
Kinetics
Simulation
Polyhydroxyalkanoate
Polyhydroxybutyrate

The Flory–Schulz distribution has long been used to describe the probability mass function of polymerization processes, enabling the calculation of polymerization kinetics. However, an equivalent distribution function for depolymerization processes remains elusive. In this study, we present a novel simulation-assisted kinetics model to investigate the depolymerization dynamics of polyhydroxybutyrate (PHB).

Our simulation replicates the random scission of a linear polymer chain and is calibrated against experimental data, yielding a conversion parameter that quantifies the extent of bond cleavage within the polymer. This conversion was then incorporated into the established pseudo second-order reaction kinetics for PHB to describe the temporal evolution of the depolymerization process.

A key assumption in the model is that oligomers with six or fewer repeating units are water-soluble and constitute the measurable depolymerization yield. The simulation provides the proportion of these small oligomers, which were fitted as a function of conversion. This relationship was integrated into the kinetics model, resulting in a predictive expression for the water-soluble yield over time.

To further simplify the application of the simulation results, we derived an analytical distribution function that approximates the fragment length distribution resulting from random chain scission. This distribution reproduces the simulation outcomes with high accuracy and enables easier application in analytical and modeling contexts. Together, the kinetics model and distribution function offer a comprehensive and practical framework for understanding and predicting polymer degradation behavior.

1. Introduction

Polymeric materials are ubiquitous across modern industries, serving critical roles in packaging, medicine, textiles, and engineering. In order to approach these rising global plastic amounts, numerous approaches for polymer recycling of commodity polymers have been developed and assessed [1–3]. In parallel with rising demand of polymeric materials, environmental concerns have prompted growing interest in biodegradable and recyclable polymers [4,5]. Among these, polyhydroxybutyrate (PHB), a member of the polyhydroxyalkanoate (PHA) family, has emerged as a promising candidate due to its biocompatibility and thermoplastic behavior [6–9]. Due to its ability of full conversion into its monomers under specific conditions, PHB has gained attention within the scope of circular economy due to ongoing research regarding its chemical recycling properties [10]. Furthermore, the PHA family is also considered to be biodegradable under environmental conditions [11].

PHB is particularly notable for its potential in closed-loop material cycles, where controlled degradation and chemical recycling can return valuable monomers or intermediates. This is due to the intrinsic chemical nature of ester bonds in PHB in contrast to commodity polyolefins, where exclusively C—C bonds form the polymer chains [12]. Numerous hydrolytic and solvolytic methods have been explored to selectively cleave such ester bonds, including acid- and base-catalyzed hydrolysis [7,13–15], methanolysis using ionic liquids [16,17], enzymatic hydrolysis [18] and aminolysis [19]. The structure of PHB, particularly its crystallinity and molar mass, significantly affects degradation kinetics, influencing both the rate and nature of hydrolysis products [6,20].

In recent years, chemical recycling approaches have gained

* Corresponding author.
E-mail address: christian.paulik@jku.at (C. Paulik).

https://doi.org/10.1016/j.polymdegradstab.2026.111949
Received 21 November 2025; Received in revised form 16 January 2026; Accepted 16 January 2026
Available online 17 January 2026

attraction. For instance, ferric chloride, zinc complexes and Brønsted acid catalysts have been used to recover crotonic acid and hydroxy acids from PHB with high yields [21–23]. These processes not only enable circular material use but also open pathways to valuable platform chemicals [12,24].

Despite this progress, the modeling of PHB degradation kinetics remains relatively underdeveloped. Classical models often apply pseudo first- or second-order reaction assumptions without capturing the underlying molecular transformations or product distributions. This stands in contrast to polymerization, where statistical distributions such as the Flory–Schulz model effectively describe molar mass distributions from first principles [25].

A notable challenge in depolymerization modeling is the stochastic nature of random chain scission. As predominantly in aliphatic polyester systems [20], polymer chains break at arbitrary positions within the polymer chain and not exclusively at the sides, a complex and evolving distribution of fragments emerges. Although some efforts have been made to correlate degradation rates with average molar mass or solubility thresholds [13,26], few studies have derived explicit fragment length distributions or integrated such distributions into kinetic models.

To address this gap, we present a simulation-assisted framework for modeling PHB depolymerization kinetics. Our approach involves calibrating a random scission simulation using experimental hydrolysis data and extracting a conversion-dependent solubility yield. Additionally, we derive an analytical distribution function that closely reproduces the simulation results and allows generalization beyond specific experimental conditions.

This dual contribution, a predictive kinetic model and a robust statistical distribution, lays the foundation for more accurate, transferable analysis of polymer degradation. It also provides a flexible toolkit for optimizing reaction conditions in chemical recycling workflows and evaluating the degradability of polymer candidates in broader sustainability efforts [27,28].

2. Experimental

2.1. Materials

PHB (ENMAT Y3000) was purchased from T&T Industry group ltd. Guangdong, China. Crotonic acid (CA) and 3-hydroxybutyric acid (3HB) were purchased from Sigma Aldrich. Formic acid and chloroform HPLC grade were purchased from Honeywell. Acetonitrile for HPLC was purchased from VWR Chemicals.

2.2. Hydrolysis in the melt

The experimental setup utilized three identical Hastelloy autoclave reactors (315 bar, 350 °C) from Dr. Thiedig & Co KG, each equipped with K-type thermocouples from TCDirect for precise temperature monitoring and pressure transducers PTD.VB400 (0 to 400 bar) from Parker Hannifin for online pressure monitoring. A Polytetrafluoroethylene (PTFE) capsule was placed inside each reactor to enhance reproducibility by minimizing metal contamination from the reactor.

2.4 *g* of PHB and 40 mL of water were added to the vessel, sealed with PTFE thread seal. The autoclaves were heated to 200 °C with 750 W heating jackets and temperature regulation was achieved using a Eurotherm 2132 PID temperature controller. During the reaction, the pressure and temperature data were processed via an ET7019Z module from ICP DAS and transmitted through modbus TCP.

After the desired reaction time, the autoclaves were cooled in a water bath to 40 °C, after which the PTFE capsules were removed, and the reaction mixture was further cooled to room temperature. The resulting mixture was filtered to separate water-soluble and insoluble products. The insoluble fraction was air-dried, while the water-soluble fraction was concentrated by rotary evaporation yielding a yellowish oil with transparent, needle-like crystals.

2.3. Characterization

The water-insoluble product fraction was analyzed via size exclusion chromatography (SEC) on an Agilent Technologies 1200 Series GPC system. Separation was achieved on 3 Phenogel columns (300×4.6 mm, 5 μm, Linear(2), 10^3 Å, and 50 Å) heated to 40 °C. As mobile phase chloroform ($CHCl_3$) was used with a flowrate of 0.35 mL min^{-1}. 50 μL of a 4 mg mL^{-1} solution in $CHCl_3$ were injected.

The water-soluble fraction was concentrated by rotary evaporation, weighed and analyzed using a high-performance liquid chromatography (HPLC) system. A Thermo Scientific Surveyor HPLC system equipped with a ZORBAX SB-C18 reversed-phase column (250×4.6 mm, 5 μm) heated to 40 °C and an Thermo Scientific Orbitrap Velos MS with atmospheric pressure chemical ionization were used. The sample injection volume was 20 μL. A solvent gradient of 0.2 mL min^{-1}, using H_2O with 0.1 % formic acid (A) and acetonitrile with 0.1 % formic acid (B) was applied. The gradient starts with 95 % A for 2 min, gradually shifting to 95 % B over 23 min, held for three minutes.

For long-term experiments (>150 min reaction time) the autoclave headspace gases were sampled into a closed glass vial. Gas samples were manually taken with a gastight syringe and 1 mL injected into a gas chromatography (GC) system (Thermo Scientific Trace GC Ultra) equipped with a thermal conductivity detector (TCD). The separation is performed using a Carboxen™-1000 packed column using helium at a flow rate of 4.5 mL min^{-1} as carrier gas. The following GC parameters were used: inlet heater 150 °C, detector 230 °C, oven initial temperature 40 °C, hold for 5 min, raise temperature at a rate of 20 °C min^{-1} to 225 °C, 10 min at final temperature.

In addition to GC-TCD, the gas samples were also analyzed using a quadrupole mass spectrometer (HPR-20 R&D – Hiden Analytical), using a 50 amu mass range option. Electron Impact ionisation was applied with an electron energy of 70 eV. For the analysis, 20 scans of the sample were performed and averaged.

2.4. Simulation

Fig. 1 provides a conceptual overview of the simulation process. The molar mass distribution of the initial polymer is first characterized using SEC, and the measured molar masses are converted into the corresponding number of repeating units (*RU*). Based on the peak intensities associated with each *RU*, the number of molecules (n) is estimated and used as input for the simulation. Given n_i simulated molecules composed of RU_i repeating units, the total number of ester bonds in the system can then be calculated using Eq. (1).

$$n_{bonds} = \sum_i n_i \cdot (RU_i - 1) \tag{1}$$

Using this value in conjunction with the conversion factor X, which represents the fraction of ester bonds that undergo scission, the total number of scission events can be calculated as:

$$n_{scissions} = n_{bonds} \cdot X \tag{2}$$

To simulate a random scission process where every ester bond has an equal probability of breaking, a weighted random selection algorithm is used. The algorithm first selects a molecule in which the scission occurs. This selection is not uniform but follows a probability distribution that is proportional to the number of ester bonds contributed by each molecular species. This distribution is given by Eq. (3):

$$P_i = \frac{n_i \cdot (RU_i - 1)}{n_{bonds}} \tag{3}$$

Here, P_i denotes the probability of selecting a molecule with RU_i repeating units, present n_i times in the system. Molecules with a larger number of ester bonds, and thus more potential scission sites, are more likely to be chosen.

Once a molecule is selected, the specific position of the bond break is

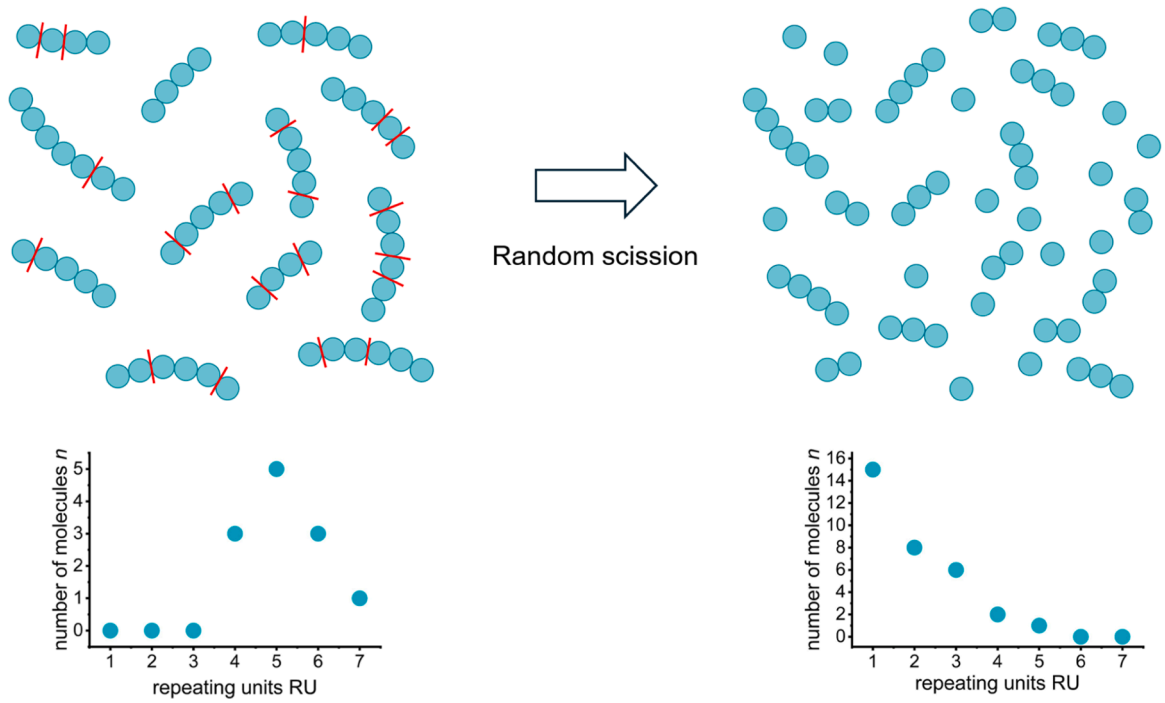

Fig. 1. Conceptual image of the simulated random scission process on a linear polymer. The initial concept polymer is converted with a conversion of 40 %.

determined by a random integer generated between 1 and RU_i-1, corresponding to a possible ester bond within the molecule. The molecule is then cleaved into two fragments: the first with RU_j repeating units (where j is equal to the randomly chosen cleavage point), and the second with $RU_k = RU_i - RU_j$ repeating units.

The simulation proceeds by adjusting the molecule count: the original molecule count n_i is decremented by one, and the counts for the two resulting fragments, n_j and n_k, are each incremented by one. This entire process including molecule selection, scission site determination, and fragment update, is repeated iteratively for a total of $n_{scission}$ cycles.

This random scission algorithm ensures a statistically accurate representation of the degradation process under the assumption of uniform bond breakage probability across the polymer population. A graphical illustration of such scission process on the initial GPC data can be found in Fig. S1 in blue in the supporting information.

To estimate the amount of water-soluble monomers and oligomers formed as a function of conversion X, it is assumed that all oligomers containing up to six repeating units are water-soluble. Based on this assumption, the simulation described above is used to determine the yield of soluble species, specifically, monomers and oligomers with up to six repeating units across a range of conversions.

It is important to note that yield, in this context, refers to the total mass of water-soluble products, not merely their number. Therefore, to convert the simulated distribution of oligomers (expressed as molecule counts per repeating unit length) into a mass-based yield, each oligomer class is weighted by its number of repeating units. In other words, the contribution of a given oligomer to the overall yield is calculated as the product of its molecule count and its chain length. This ensures that longer oligomers, which contribute more to the total mass, are appropriately represented in the yield.

Fig. 2 displays the results of these simulations and a sigmoidal fit for the total yield of water-soluble fragments. The cumulative yield of water-soluble fragments up to six repeating units exhibits a sigmoidal trend, which is well-described by the following empirical expression:

$$Y_{WS} = 1 - \frac{1.2089}{1 + e^{\frac{X-0.1925}{0.109}}} \quad (4)$$

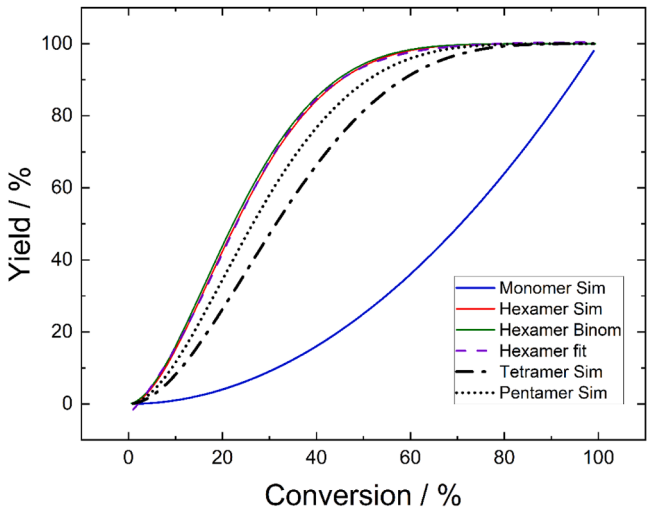

Fig. 2. Mass yield of monomers and cumulative oligomers resulting from ester bond conversion. The yield for the cumulative oligomers includes all species with 4–6 repeating units or fewer. Simulation as described in Section 2.4, 'Binom'-distribution as described in Section 3.1, including the sigmoidal fit from (eq. (4)) in purple.

Here, Y_{WS} represents the total yield of water-soluble species as a function of conversion X. This relationship arises purely from statistical considerations based on the random scission of polymer chains. It reflects the increasing probability of forming small, soluble fragments as more bonds are cleaved, which agrees with findings from literature, even though they use a methodically different Monte-Carlo approach [29,30].

3. Theory and calculation

3.1. Distribution function

As already shown by Charlesby & Freeth [31] for the random scission of polymers about five fractures per molecule are needed so that the starting distribution is not important any more. Bearing that in mind and building on the principles outlined in the simulation section above, a distribution function was developed to describe the probability of fragment lengths resulting from random scission. Specifically, a discrete solution was derived for the special case of a single linear polymer chain of length L undergoing n random cuts. A figurative description of this issue is depicted in the supporting information in yellow in Fig. S1. The resulting probability P_n of obtaining a fragment of length x is given by the expression based on binomial coefficients:

$$P_n = \frac{\binom{L-x}{n} - \binom{L-x-1}{n}}{\binom{L-1}{n}} \tag{5}$$

Eq. (5) represents a special case: it describes the statistical outcome of cutting a single chain of length L, n times at random positions. While this idealized model involves only one chain, it can be used to approximate real-world polymer degradation, where a broad molar mass distribution is typically present. To extend this model to practical systems, one can relate the chain length L to experimental data by:

- Estimating the initial chain length L from the number-average molecular weight M_n measured by SEC, using:

$$L = \frac{M_n}{M} \tag{6}$$

Where M is the molar mass of the repeating unit, in case of PHB 86.09 $g\ mol^{-1}$.

- Determining the number of scission events n from the bond conversion X, assuming a linear chain:

$$n = X \cdot L \tag{7}$$

- Calculating the resulting fragment lengths x from the distribution P_n, which gives the probability of a fragment of length x being formed after n random cuts to a chain of length L.

By comparing the single-chain distribution model with the simulation connecting to experimental parameters, the derived probability function serves as a useful approximation for simulating the fragment length distributions in realistic polymer degradation scenarios, as depicted in Fig. S1. This is also illustrated in the marginal differences of the different approaches (red, green and purple line) in Fig. 2.

3.2. Kinetics

The depolymerization process under study in principle follows a third order kinetics, where the concentrations of the ester bonds [E], the acid groups [A] and water [H_2O] as the nucleophile are considered. Due to the use of water in excess, the present study considers the depolymerization as pseudo second-order reaction kinetics, as previously described and derived by Antheunis *et al.* [32]. Specifically, the concentration of carboxylic acid end groups [A], formed as a result of ester bond hydrolysis, evolves over time according to the following expression:

$$[A] = [A]_0 \cdot \frac{e^{c_1 \cdot t} - 1}{\frac{[A]_0}{[E]_0} \cdot e^{c_1 \cdot t} + 1} \tag{8}$$

The step-by-step derivation of this equation has been published by Antheunis *et al.* [32] and in the respective supporting information. Here, $[A]_0$ is the initial concentration of carboxylic acid groups and $[E]_0$ is the initial concentration of ester bonds. The term c_1 is defined as:

$$c_1 = ([A]_0 + [E]_0) \cdot k_H \tag{9}$$

Where k_H is the rate coefficient for the hydrolysis of ester bonds.

Since each hydrolyzed ester bond leads to the formation of a carboxylic acid group, the concentration [A] can also be interpreted as the number of converted ester bonds. Some literature assumes polymer degradation to follow pseudo-first-order kinetics only depending on the [E]. Nevertheless, this special case is only valid under excess of [H_2O], low conversions, so that [A] is still negligibly small for non-catalytic depolymerization reactions [33]. However, this relation between [A] and conversion allows us to define the conversion of ester bonds, denoted by X, as the fraction of ester bonds that have reacted:

$$X = \frac{[A]}{[E]_0} = \frac{[A]_0}{[E]_0} \cdot \frac{e^{c_1 \cdot t} - 1}{\frac{[A]_0}{[E]_0} \cdot e^{c_1 \cdot t} + 1} \tag{10}$$

This equation enables the calculation of the conversion X as a function of time, based on initial concentrations and the hydrolysis rate coefficient. It serves as a key link between the reaction kinetics and the simulation framework described in the previous sections.

3.3. Accounting for side reaction

In addition to ester bond hydrolysis, a side reaction namely the decarboxylation of acid groups must be considered. This reaction has been described by Li & Strathmann [34], and is depicted with the following scheme 1:

As described in literature, 3-hydroxy butyric acid (3HB) and crotonic acid (CA) are in an equilibrium at elevated temperatures via addition or elimination of water. This side reaction is modeled here using first-order kinetics with the rate of decarboxylation summarized given by:

$$r = -\frac{d[M]}{dt} = k_s \cdot [M] \tag{11}$$

Where [M] is the concentration of decarboxylation-prone monomers, and k_s is the rate coefficient for the side reaction. To estimate the carboxylic acid group concentration from the simulation, the concentration of acid [A] is related to the conversion as:

$$[M] = [E]_0 \cdot X \tag{12}$$

This means, that regarding the side reaction a linear relationship between conversion and yield of monomer [M] is assumed. Combining Eqs. (11) and (12) gives:

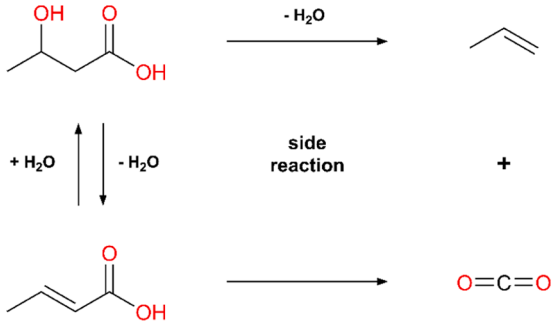

Scheme 1. Chemical reaction of the decarboxylation reaction including the equilibrium of 3HB and CA.

$$-\frac{d[M]}{dt} = k_s \cdot [E]_0 \cdot X \tag{13}$$

To connect this side reaction with the main hydrolysis pathway, the total converted ester bonds [A] from Eq. (8) are used, leading to a derived expression for the change in monomer concentration due to decarboxylation:

$$\Delta[M] = k_s \cdot \frac{ln([E]_0 + [A]_0 \cdot e^{c_1 \cdot t})}{k_H} - [A]_0 \cdot k_s \cdot t + C_{int} \tag{14}$$

where the integration constant C_{int} is determined by the initial condition at $t = 0$:

$$C_{int} = -k_s \cdot \frac{ln([E]_0 + [A]_0)}{k_H} \tag{15}$$

The side reaction contribution to the overall yield is expressed as a normalized conversion:

$$X_{side} = \frac{\Delta[M]}{[E]_0} \tag{16}$$

The final observable water-soluble yield Y is obtained by subtracting this side reaction contribution from the water-soluble species predicted by the main simulation:

$$Y = Y_{WS} - X_{side} \tag{17}$$

Finally, a combined model for the full system accounting for both main-chain hydrolysis and monomer degradation via decarboxylation is given by:

$$Y = 1 - \frac{1.2089}{1 + e^{\frac{\frac{[A]_0}{[E]_0}\frac{e^{c_1 \cdot t} - 1}{e^{c_1 \cdot t} + 1} - 0.1925}{0.109}}} - \frac{\frac{k_s \cdot ln([E]_0 + [A]_0 \cdot e^{c_1 \cdot t}) \cdot ([A]_0 + [E]_0)}{c_1} - [A]_0 \cdot k_s \cdot t - \frac{k_s \cdot ln([E]_0 + [A]_0)}{k_H}}{[E]_0} \tag{18}$$

This full model captures both the yield of water-soluble products due to ester hydrolysis (main reaction) and the irreversible degradation of monomers to gaseous products (side reaction), allowing for more accurate prediction of water-soluble product formation under various experimental conditions. For a more detailed description of equation (18)please refer to Scheme S1 in the supporting information.

4. Results and discussion

As described in Section 3.1, the first analysis approach was the investigation of the solid residues after the melt hydrolysis experiments via SEC. The displayed results in Fig. S2 of the supporting information reveal no clear trend within the selected reaction time scales, but are in good agreement with SEC data of recent work [35]. Here, even after one hour of melt hydrolysis, the resulting M_n is rather small ($\sim$1000 $g\,mol^{-1}$) which was expected from the mechanism of bulk erosion in contrast to surface erosion processes [13,29]. In order to access degradation products with higher molar masses, significantly shorter reaction times would be required. Due to the high thermal mass of our autoclave setup used, these could not be achieved in a reliable way, which was a major motivation for the development of the present simulation and kinetic modelling.

In order to evaluate the experimental results from the melt hydrolysis runs, the fraction of water-soluble products was collected and purified. Exactly these yields were used as input data for the model and tool derived in Section 3. Based on them as well as the initial molar mass distribution, the conversion X, development of the M_n, Y_{ws} and the yield for the side reaction X_{side} were fitted and calculated, as depicted in the following Fig. 3:

Fig. 3 shows the fit achieved for the yield as well as the conversion of the side reaction and the predicted number average molar mass. The blue dots in Fig. 3 display the measured SEC data, which are in good agreement with the modeled progress of M_n from the simulation. As expected from literature reports [13] on such bulk degradation processes, the major decrease in molar mass was predicted for the first 25 min of reaction time.

The red dots depict the experimental yield values of water-soluble products. Again, they are in good agreement with the modeled

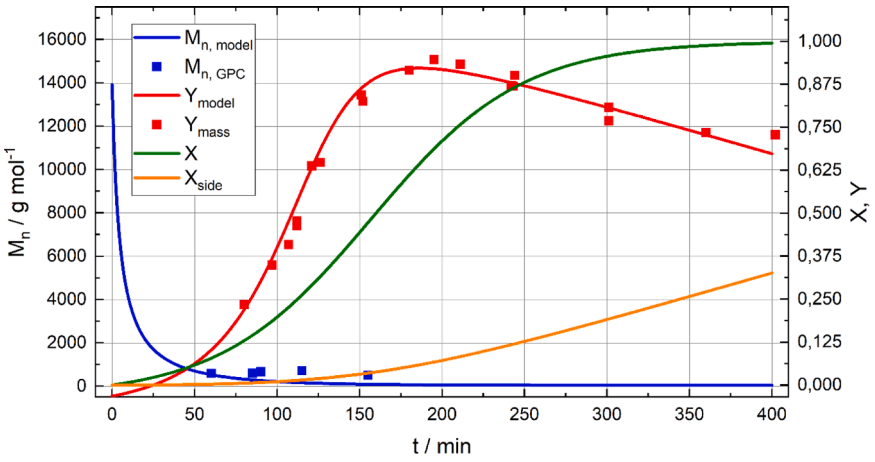

Fig. 3. Comparison of the developed model with experimental data for the water-soluble yield during PHB hydrolysis in the melt. X represents the conversion of ester bonds, X_{side} accounts for the conversion of monomers into gaseous products via decarboxylation, and Y is the predicted water-soluble yield according to the full model described in this work. The number-average molecular weight M_n was measured via SEC, and conversion was modeled using the autocatalytic equation reported by Antheunis *et al.* [32].

progress curve shown in red, which exhibits a maximum at 186 min. A direct comparison to literature results is not possible, as in this work all water-soluble monomers and oligomers are considered. The existence of oligomeric species in addition to monomers was qualitatively proven via HPLC, as depicted in Fig. S3 in the supporting information.

With an increase in the side reaction, shown as orange line in Fig. 3, a decrease of the water-soluble yield after the maximum point was observed. The side reaction (Scheme 1) is not only visible in the missing yield of the water-soluble product but since two gas molecules per decarboxylated monomer are produced, also a significant pressure increase was observed during melt hydrolysis reactions. In addition to this pressure increase, the relative headspace composition after the experiments was analyzed and is depicted in the supporting information in Fig. S4. A more detailed analysis of the datapoints recorded as triplicates including relative errors in Table S1 revealed a decrease in air content, which was accompanied by an increase in CO_2 and propene content. These two gases were detected nearly in a 1:1 ratio, as deduced from Scheme 1. As a result of the solubility of CO_2 in the aqueous reaction medium, the concentrations of [CO_2] were persistently smaller than those of [propene], which was also reported in literature for degradation studies of pure monomer [34]. Considering the sum of the products analyzed revealed values close to 100 %.

In addition to the graphical illustration shown in Fig. 3, the developed model was evaluated by fitting for $[A]_0$, k_H and k_s experimental data on the hydrolytic degradation of PHB in the melt phase. Fitting Eq. (18) through least square method to the measured yields of the experiments gives:

$[A]_0 = 8.29{\cdot}10^{-4}\ M$	$\sigma_{[A]_0} = \pm 1.888{\cdot}10^{-4}$
$k_H = 0.783\ M\ min^{-1}$	$\sigma_{k_H} = \pm 0.053$
$k_s = 1.36{\cdot}10^{-3}\ M$	$\sigma_{k_s} = \pm 7.38{\cdot}10^{-5}$

As in addition to the simple fitting values, also a covariance matrix was calculated, which enabled the estimation of standard deviations of the results. From a view at Fig. 3, a good correlation can be deduced, which is reflected by quite low relative errors for both rate coefficients of around six percent. For the fit of the initial concentration of acid groups $[A]_0$ a larger error was obtained.

The initial acid concentration calculated by this fit is two orders of magnitude smaller than expected using the assumptions made in the supporting information of Antheunis *et al.* [32] which was $[A]_0 = 9.03{\cdot}10^{-2}\ mol\ L^{-1}$.

One reason for this difference is the approach of how the acidity of carboxylic acid groups is accounted. In our calculation based on Antheunis, all carboxylic acid groups are counted. However, the value from the simulation fit is accounting for the actual catalytically active carboxylic acid groups, where the chemical activity and dissociation constant of the acids is also considered. For example, Laycock *et al.* [29] reports a kinetic model, where this degree of dissociation is also considered.

In order to compare the result of the rate coefficient for the side reaction k_s with literature data, values from the following reports on decarboxylation were chosen, although some assume a different reaction mechanism. Gubatanga *et al.* [36] reported decarboxylation reactions of CA and butyric acid (BA), however at temperatures above 300 °C. Bigley & Clarke [37] performed detailed studies on CA and its isomerization and decarboxylation reaction at 360 °C. As third literature reference, the data for the decarboxylation of 3HB of Li & Strathmann [34] was selected.

As depicted in Fig. 4, the literature values for decarboxylation of CA and BA show significant deviation from the value derived in this work. Comparing the reaction rate coefficient for the side reaction to Li & Strathmann [34] who calculated the decarboxylation for 3HB resulted in a close hit, with the results from the linear fit displayed in Table S2. This indicated that the rate of the side reaction is close to the decarboxylation of 3HB in terms of kinetics, which is expected as 3HB is reported in literature to be the primary monomeric product under comparable conditions.

Care has to be taken for a direct comparison of the reaction rate coefficient for the hydrolysis to literature since our approach of using the individual ester bonds in combination with the distribution function/simulation for calculation is based on a novel model. However, as the rate coefficient for the decarboxylation in Fig. 4 was in good agreement to the work of Li & Strathmann [34], a similar comparison to their data was done using the rate coefficient for the hydrolysis. In order to do so, their data was re-calculated using Eq. (4) from the present work. As the M_n in their case is unknown, the assumption of using the same value as in our study was made. We are aware, that this assumption introduces a significant uncertainty which has to be kept in mind interpreting the following results:

The data points in squares in Fig. 5 were recalculated from the study results of Li & Strathmann [34]. With the exception of the datapoint recorded at 175° (marked in blue), their rate coefficients show a good linear relationship in this Arrhenius plot. The results of this Arrhenius analysis are shown in Table S3, which show however less linearity compared to the analysis of the side reaction rate coefficient in Table S2.

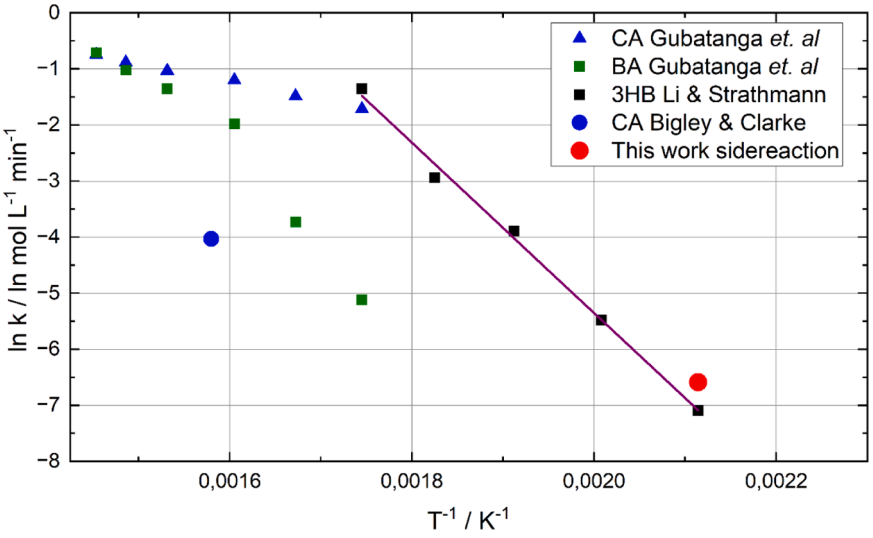

Fig. 4. Comparing the calculated reaction coefficient vs. rate coefficients of decarboxylation reactions from literature in an Arrhenius plot. CA and BA from Gubatanga *et al.* [36], CA from Bigley & Clarke [37] and 3HB from Li & Strathmann [34].

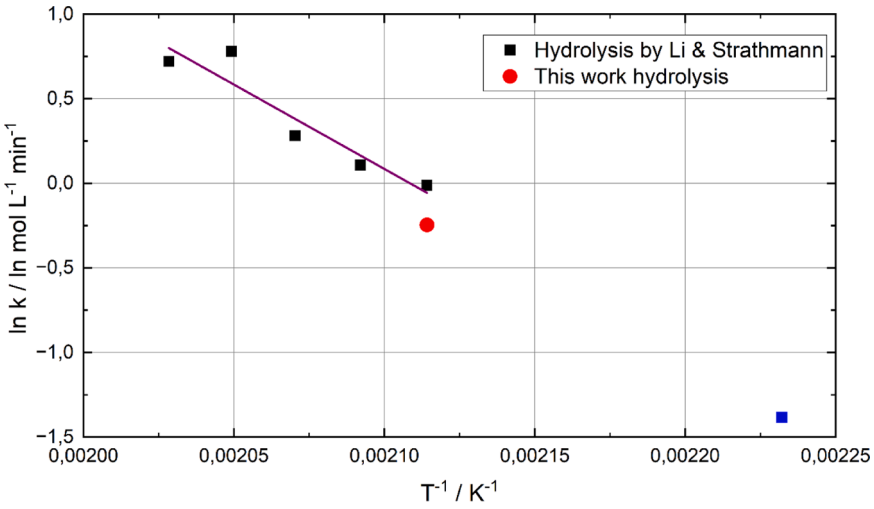

Fig. 5. Comparing the calculated reaction coefficient vs. rate coefficients of polyester hydrolysis reactions from literature of Li & Strathmann [34] in an Arrhenius plot. the blue square reflects the literature data at 175 °C, which was not considered for the illustration of linearity in the purple line.

In comparison, the red point marks the rate coefficient for the hydrolysis reaction obtained by the fit depicted in Fig. 3. Although a difference to the literature data is observed, based on the standard deviation and the assumptions made the relation shown in Fig. 5 can be interpreted as a good match. In addition, the work by Saeki *et al.* [13] depicts a similar Arrhenius plot for the hydrolytic degradation coefficients of PHB also. Although the lack of data values complicates a quantitative comparison, the graphs are in good agreement to our calculated data.

In a further attempt, our model was applied using the literature data and regressions from Fig. 4 and Fig. 5 to predict the yields of monomers, oligomers and overall water-soluble yield, as depicted in Fig. S5. Regarding the water-soluble yield, a good agreement with the data from Li & Strathmann was achieved, however larger deviations regarding the monomer and oligomer yield were observed. Following this analysis based on literature data, it appears that the monomer content was underestimated while the oligomer content was overestimated. In order to achieve a full model regarding temperature dependence in the future, on the one hand further experimental data (using known M_n) and on the other hand in-depth knowledge of the quantity and nature of the oligomeric fraction are required.

5. Conclusions

In this work, a novel kinetic approach for a random scission depolymerization of linear polyesters via hydrolysis was derived. A detailed knowledge of kinetic steps of depolymerization of polyhydroxybutyrate (PHB) as a model case, including the decarboxylation reaction of the monomers regarded as side reaction was the foundation for the experimental studies performed. Using the validated assumption, that oligomers up to six repeating units are water-soluble, the yield of water-soluble products was chosen as key parameter for the present work. Mathematical fitting of the kinetic model using our experimental data yielded in a very good validation of the model and kinetic data of the initial carboxylic acid concentration $[A]_0$, the rate coefficient for the hydrolysis k_H and the rate coefficient for the side reaction k_s. Thereby the connection between kinetic formulae and reaction time was done via the mathematical distribution function showing excellent fitting results, rather than Monte Carlo methods frequently reported elsewhere in literature. Especially our value of k_s of 1.36×10^{-3} M is in excellent agreement with literature data. Furthermore, the quantification of a steadily increase in pressure upon reaction time caused by a decarboxylation reaction yielding CO_2 and propene in a 1:1 ratio was proven to follow the mechanism according to literature.

Due to the novelity of our approach, a direct comparison of the k_h with literature is demanding. In an attempt using assumptions and recalculating literature data from Li & Strathmann a good validity of our model was demonstrated. Upon further research on different rection conditions and in-depth analysis of the exact composition of the monomers and oligomers formed in the water-soluble hydrolysate will pave the path for future application of our model in a broader context. In-depth knowledge on chemical depolymerization routes of biopolymers like PHA, as demonstrated in this work, will contribute to the accelerated development of circular economy routes.

Author information

All authors have approved the final version of the manuscript.

CRediT authorship contribution statement

Norbert Hohenauer: Writing – original draft, Visualization, Validation, Software, Methodology, Investigation, Formal analysis, Data curation. **Dominik Wielend:** Writing – original draft, Visualization, Investigation. **Katharina Kelderer:** Writing – review & editing, Investigation. **Jan-Michael Holzinger:** Investigation, Formal analysis. **Gunnar Spiegel:** Writing – review & editing, Supervision, Project administration, Funding acquisition, Conceptualization. **Clemens Schwarzinger:** Writing – review & editing, Investigation. **Christian Paulik:** Writing – review & editing, Supervision, Resources, Funding acquisition.

Declaration of competing interest

The authors declare that they have no known competing financial interests or personal relationships that could have appeared to influence the work reported in this paper.

Acknowledgement

This research was conducted as part of the cooperation project "BIOCYCLE-UA II | Kreislaufwirtschaft am Beispiel von ausgewählten Biopolymeren (Herstellung -Verarbeitung-Recycling)", co-funded by the European Union within the IBW/EFRE & JTF 2021–2027 program „Investitionen in Beschäftigung & Wachstum/ EFRE & JTF 2021–2027", Österreich.

This work was conducted as part of the COMET Center CHASE, funded within the COMET – Competence Centers for Excellent Technologies programme by the BMIMI, the BMWET and the Federal

Provinces of Upper Austria and Vienna. The COMET programme is managed by the Austrian Research Promotion Agency (FFG).

The authors thank Simon Herber and Florian Kühberger (Competence Center CHASE GmbH) for their support and help with the Hiden Analytics mass spectrometer.

Discussions regarding distribution functions with Christoph Koutschan and Josef Schicho (Research Institute for Symbolic Computation – RISC) is kindly acknowledged.

The open access publication of this work is supported by the Johannes Kepler Open Access Publishing Fund and the federal state Upper Austria.

Supplementary materials

Supplementary material associated with this article can be found, in the online version, at doi:10.1016/j.polymdegradstab.2026.111949.

Data availability

Data will be made available on request.

References

[1] T. Uekert, A. Singh, J.S. DesVeaux, T. Ghosh, A. Bhatt, G. Yadav, S. Afzal, J. Walzberg, K.M. Knauer, S.R. Nicholson, G.T. Beckham, A.C. Carpenter, Technical, economic, and environmental comparison of closed-loop recycling technologies for common plastics, ACS Sustain. Chem. Eng. 11 (2023) 965–978, https://doi.org/10.1021/acssuschemeng.2c05497.

[2] I.A. Ignatyev, W. Thielemans, B. VanderBeke, Recycling of polymers: a review, ChemSusChem 7 (2014) 1579–1593, https://doi.org/10.1002/cssc.201300898.

[3] T. Rumetshofer, J. Fischer, Information-based plastic material tracking for circular economy—a review, Polymers 15 (2023) 1623, https://doi.org/10.3390/polym15071623.

[4] N. Singh, T.R. Walker, Plastic recycling: a panacea or environmental pollution problem, NPJ Mater. Sustain. 2 (2024) 17, https://doi.org/10.1038/s44296-024-00024-w.

[5] G.X. De Hoe, T. Şucu, M.P. Shaver, Sustainability and polyesters: beyond metals and monomers to function and fate, Acc. Chem. Res. 55 (2022) 1514–1523, https://doi.org/10.1021/acs.accounts.2c00134.

[6] F. Kučera, J. Petruš, J. Jančář, The structure-hydrolysis relationship of poly(3-hydroxybutyrate), Polym. Test. 80 (2019) 106095, https://doi.org/10.1016/j.polymertesting.2019.106095.

[7] G. Yu, R.H. Marchessault, Characterization of low molecular weight poly (β-hydroxybutyrate)s from alkaline and acid hydrolysis, Polymer 41 (2000) 1087–1098, https://doi.org/10.1016/S0032-3861(99)00230-X.

[8] A. Chamas, H. Moon, J. Zheng, Y. Qiu, T. Tabassum, J.H. Jang, M. Abu-Omar, S. L. Scott, S. Suh, Degradation rates of plastics in the environment, ACS Sustain. Chem. Eng. 8 (2020) 3494–3511, https://doi.org/10.1021/acssuschemeng.9b06635.

[9] M. Zhou, M. Edeleva, G. Wang, L. Cardon, D.R. D'hooge, Reactive blending of deliberately degraded polyhydroxy-butyrate with poly(lactic acid) and maleic anhydride to enhance biopolymer mechanical property variations, Eur. Polym. J. 230 (2025) 113890, https://doi.org/10.1016/j.eurpolymj.2025.113890.

[10] R.W. Clarke, G. Rosetto, T. Uekert, J.B. Curley, H. Moon, B.C. Knott, J. E. McGeehan, K.M. Knauer, Polyhydroxyalkanoates in emerging recycling technologies for a circular materials economy, Mater. Adv. 5 (2024) 6690–6701, https://doi.org/10.1039/D4MA00411F.

[11] M. Koller, D. Heeney, A. Mukherjee, Biodegradability of polyhydroxyalkanoate (PHA) biopolyesters in nature: a review, Biodegradation 36 (2025) 76, https://doi.org/10.1007/s10532-025-10164-y.

[12] R.A. Clark, M.P. Shaver, Depolymerization within a circular plastics system, Chem. Rev. 124 (2024) 2617–2650, https://doi.org/10.1021/acs.chemrev.3c00739.

[13] T. Saeki, T. Tsukegi, H. Tsuji, H. Daimon, K. Fujie, Hydrolytic degradation of poly [(R)-3-hydroxybutyric acid] in the melt, Polymer 46 (2005) 2157–2162, https://doi.org/10.1016/j.polymer.2005.01.030.

[14] V. Jašek, J. Fučík, L. Ivanová, D. Veselý, S. Figalla, L. Mravcova, P. Sedlacek, J. Krajčovič, R. Přikryl, High-pressure depolymerization of poly(lactic acid) (PLA) and poly(3-hydroxybutyrate) (PHB) using bio-based solvents: a way to produce alkyl esters which can Be modified to polymerizable monomers, Polymers 14 (2022) 5236, https://doi.org/10.3390/polym14235236.

[15] Q. Zhang, Y. Wang, G. Xu, R. Yang, R. Li, Q. Wang, Organocatalytic depolymerization of poly(3-hydroxybutyrate) to crotonic acid, Polym. Degrad. Stab. 218 (2023) 110591, https://doi.org/10.1016/j.polymdegradstab.2023.110591.

[16] X. Song, H. Wang, F. Liu, S. Yu, Kinetics and mechanism of monomeric product from methanolysis of poly (3-hydroxybutyrate) catalyzed by acidic functionalized ionic liquids, Polym. Degrad. Stab. 130 (2016) 22–29, https://doi.org/10.1016/j.polymdegradstab.2016.05.023.

[17] X. Song, F. Liu, H. Wang, C. Wang, S. Yu, S. Liu, Methanolysis of microbial polyester poly(3-hydroxybutyrate) catalyzed by Brønsted-Lewis acidic ionic liquids as a new method towards sustainable development, Polym. Degrad. Stab. 147 (2018) 215–221, https://doi.org/10.1016/j.polymdegradstab.2017.12.009.

[18] A. Kovalcik, S. Obruca, M. Kalina, M. Machovsky, V. Enev, M. Jakesova, M. Sobkova, I. Marova, Enzymatic hydrolysis of poly(3-Hydroxybutyrate-co-3-Hydroxyvalerate) scaffolds, Materials 13 (2020) 2992, https://doi.org/10.3390/ma13132992.

[19] A.N. Boyandin, V.A. Bessonova, N.L. Ertiletskaya, A.A. Sukhanova, T.A. Shalygina, A.A. Kondrasenko, Aminolysis of poly-3-hydroxybutyrate in N,N-dimethylformamide and 1,4-dioxane and formation of functionalized oligomers, Polymers 14 (2022) 5481, https://doi.org/10.3390/polym14245481.

[20] L.N. Woodard, M.A. Grunlan, Hydrolytic degradation and erosion of polyester biomaterials, ACS Macro Lett. 7 (2018) 976–982, https://doi.org/10.1021/acsmacrolett.8b00424.

[21] X. Song, C. Wang, Y. Shen, F. Liu, S. Yu, X. Ge, Methanolysis of poly(3-hydroxybutyrate) catalyzed by ferric chloride, Adv. Polym. Technol. 37 (2018) 2915–2921, https://doi.org/10.1002/adv.21963.

[22] A. Parodi, A. Jorea, M. Fagnoni, D. Ravelli, C. Samorì, C. Torri, P. Galletti, Bio-based crotonic acid from polyhydroxybutyrate: synthesis and photocatalyzed hydroacylation, Green Chem. 23 (2021), https://doi.org/10.1039/D1GC00421B.

[23] Y. Wang, R. Yang, G. Xu, X. Guo, B. Dong, Q. Zhang, R. Li, Q. Wang, Zn-catalyzed coordination-insertion depolymerization strategy of poly(3-hydroxybutyrate) under bulk conditions, Polym. Degrad. Stab. 214 (2023) 110413, https://doi.org/10.1016/j.polymdegradstab.2023.110413.

[24] V. Elhami, M.A. Hempenius, B. Schuur, Crotonic acid production by pyrolysis and vapor fractionation of mixed microbial culture-based poly(3-hydroxybutyrate-co-3-hydroxyvalerate), Ind. Eng. Chem. Res. 62 (2023) 916–923, https://doi.org/10.1021/acs.iecr.2c03791.

[25] P.J. Flory, Molecular size distribution in linear condensation polymers, J. Am. Chem. Soc. 58 (1936) 1877–1885, https://doi.org/10.1021/ja01301a016.

[26] J. Yu, D. Plackett, L.X.L. Chen, Kinetics and mechanism of the monomeric products from abiotic hydrolysis of poly[(R)-3-hydroxybutyrate] under acidic and alkaline conditions, Polym. Degrad. Stab. 89 (2005) 289–299, https://doi.org/10.1016/j.polymdegradstab.2004.12.026.

[27] A. Parodi, M. D'Ambrosio, L. Mazzocchetti, G.A. Martinez, C. Samorì, C. Torri, P. Galletti, Chemical recycling of polyhydroxybutyrate (PHB) into bio-based solvents and their use in a circular PHB extraction, ACS Sustain. Chem. Eng. 9 (2021) 12575–12583, https://doi.org/10.1021/acssuschemeng.1c03299.

[28] C. Samorì, G.A. Martinez, L. Bertin, G. Pagliano, A. Parodi, C. Torri, P. Galletti, PHB into PHB: recycling of polyhydroxybutyrate by a tandem "thermolytic distillation-microbial fermentation" process, Resour. Conserv. Recycl. 178 (2022) 106082, https://doi.org/10.1016/j.resconrec.2021.106082.

[29] B. Laycock, M. Nikolić, J.M. Colwell, E. Gauthier, P. Halley, S. Bottle, G. George, Lifetime prediction of biodegradable polymers, Prog. Polym. Sci. 71 (2017) 144–189, https://doi.org/10.1016/j.progpolymsci.2017.02.004.

[30] A. Hill, W. Ronan, A kinetic scission model for molecular weight evolution in bioresorbable polymers, Polym. Eng. Sci. 62 (2022) 3611–3630, https://doi.org/10.1002/pen.26131.

[31] A. Charlesby, F.A. Freeth, Molecular-weight changes in the degradation of long-chain polymers, Proc. R. Soc. Lond. A. Math. Phys. Sci. 224 (1954) 120–128, https://doi.org/10.1098/rspa.1954.0145.

[32] H. Antheunis, J.-C. van der Meer, M. de Geus, A. Heise, C.E. Koning, Autocatalytic equation describing the change in molecular weight during hydrolytic degradation of aliphatic polyesters, Biomacromolecules 11 (2010) 1118–1124, https://doi.org/10.1021/bm100125b.

[33] A.N. Ford Versypt, D.W. Pack, R.D. Braatz, Mathematical modeling of drug delivery from autocatalytically degradable PLGA microspheres — a review, J. Control. Release. 165 (2013) 29–37, https://doi.org/10.1016/j.jconrel.2012.10.015.

[34] Y. Li, T.J. Strathmann, Kinetics and mechanism for hydrothermal conversion of polyhydroxybutyrate (PHB) for wastewater valorization, Green Chem. 21 (2019) 5586–5597, https://doi.org/10.1039/C9GC02507C.

[35] K. Kruta, J. Fischer, P. Denifl, C. Paulik, Effect of different washing conditions on the removal efficiency of selected compounds in biopolymers, CTR 3 (2023) 134–147, https://doi.org/10.3934/ctr.2023009.

[36] D.V. Gubatanga, O. Sawai, T. Nunoura, Reaction kinetics and pathways of crotonic acid conversion in sub- and supercritical water for renewable fuel production, React. Chem. Eng. 7 (2022) 376–386, https://doi.org/10.1039/D1RE00435B.

[37] D.B. Bigley, M.J. Clarke, Studies in decarboxylation. Part 14. The gas-phase decarboxylation of but-3-enoic acid and the intermediacy of isocrotonic (cis-but-2-enoic) acid in its isomerisation to crotonic (trans-but-2-enoic) acid, J. Chem. Soc. Perkin Trans. 2 (1982) 1, https://doi.org/10.1039/p29820000001.